# A Floating Double Probe Method for Measurements in Gas Discharges

E. O. JOHNSON AND L. MALTER
*RCA Laboratories Division, Radio Corporation of America, Princeton, New Jersey*
(Received March 14, 1950)

Measurements with a Langmuir probe in varying or decaying plasmas are defeated by the fact that the plasma potential in these cases follows that of the most positive electrode it can contact. The difficulties can be obviated by the use of a pair of probes joined by a variable potential source. The double probe system "floats" with respect to the discharge system.

From the measurements of probe current *vs.* differential probe voltage, electron temperature and plasma densities can be determined. The method is also applicable to "going" discharges where it has the advantage over the single probe of exerting a negligible influence on the discharge.

## I. INTRODUCTION

IN gas discharges either of the stationary or time-varying type it is generally the case that the electrons present in the plasma regions have a Maxwellian distribution. If this is so the concept of temperature can be associated with the electrons. The electron temperature is denoted by $T_e$.

Knowledge of the electron temperature is of importance in the determination of such quantities as the ambipolar diffusion coefficients. Langmuir and Mott-Smith[1] have described a single probe technique for measuring electron temperatures as well as of other quantities such as electron density and wall and space potentials. Their method can be used for stationary and for certain types of time-varying discharges. However, in any case, unless its area is extremely small, the probe may draw sufficient electron current when operated close to space potential to disturb the discharge conditions which it is designed to measure. As will be made clear below, the single probe method (SPM), is quite unsuited for such cases as the decaying plasma which is present following the interruption of a discharge. A double probe method (DPM) has been developed which exerts a negligible influence on a discharge and which seems to yield accurate temperature data in all types of discharges, including a decaying plasma. Reifman and Dow[2] have described a double probe method for measurements in the ionosphere. Their work will be discussed below.

## II. CONSIDERATIONS REGARDING THE SINGLE PROBE METHOD (SPM)

In the Langmuir single probe method,[1] a planar, cylindrical, or spherical electrode is immersed in a discharge plasma and the current to it measured as a function of its potential. Three fairly distinct regions are observed: (1) A region of positive ion current only. In this region the current increases slowly with increasingly negative potential on the probe. (2) A region in which the current passes through zero and then increases rapidly with increasingly positive potentials. A plot of the logarithm of the electron current in this region *vs.* probe potential yields a value for the electron temperature $T_e$, (3) A region of electron current only in which the current increases slowly with increasingly positive potentials.

In region 2, the current can be expressed as:

$$\ln i_e = -(e/kT_e)V + \ln A j_0, \qquad (1)$$

where $i_e$ is the electron probe current, $j_0$ is the random electron current density, $A$ is the probe area, $T_e$ is the electron temperature.

In Eq. (1) $V$ is the plasma potential measured with respect to the probe. This infers a knowledge of the plasma potential. In practice this need not be known, since it can be replaced by its equivalent $V_S - V_p$, where $V_S$ is the cathode-plasma potential and $V_p$ is the cathode-probe potential. Equation (1) then becomes:

$$\ln i_e = (e/kT_e)V_p + \ln A j_0 - (eV_S/kT_e). \qquad (2)$$

Thus it is merely necessary to plot $\ln i_e$ *vs.* $V_p$ in order to secure a value for $T_e$. An examination of (2) reveals some possible difficulties with the SPM. Equation (2) is significant only if $V_S$, $T_e$, and $j_0$ do not change with $V_p$. In actual practice, as $i_e$ increases one often observes changes in the discharge patterns, particularly if $i_e$ is an appreciable fraction of the discharge current. Under these circumstances, the probe is disturbing, to some extent, the very quantities it is intended to measure. It would definitely be more satisfying if measurements could be made in a manner less likely to disturb the quantities it is intended to measure. As will be seen, in the double probe method the total current to the probe can never exceed the positive ion current to them. Since this positive ion current is hundreds of times smaller than the electron current to a single probe the DPM appears to be advantageous in this respect.

Langmuir and Mott-Smith[1] have shown how in addition to electron temperature, the probe data can yield values for electron and ion densities; space and wall potentials and for random electron currents. The objections cited above for the use of the SPM in electron temperature determinations are equally applicable here.

[1] I. Langmuir and H. M. Mott-Smith, Gen. Elec. Rev. **27**, 449, 538, 616, 762, 810 (1924).
[2] A. Reifman and W. G. Dow, Phys. Rev. **76**, 987 (1949).

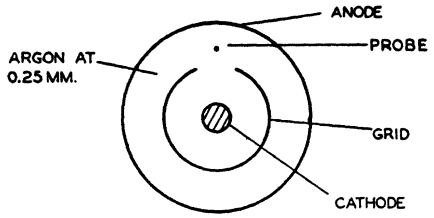


FIG. 1. Section through experimental tube for measuring floating potential of probe in decaying plasma.

## III. POTENTIAL PROPERTIES OF A DECAYING PLASMA

Consider a region enclosed by a unipotential boundary of any shape whatsoever and suppose that at time zero the region is filled with a plasma of arbitrary density distribution. What is the behavior of the plasma at later times if there is no further ionization? It is obvious that, due to their greater velocity, electrons will begin to pour out into the bounding walls. However, as this occurs, the plasma potential will rise. This will, in turn, soon prevent the further loss of all but the fastest electrons, (as determined by the Boltzmann relation). The rate of loss of electrons will diminish to equal that of the rate of loss of positive ions. The plasma now decays while retaining its plasma-like characteristics. In low pressure discharges the losses of charged particles are by the process of diffusion. The plasma potential will be slightly positive with respect to that of the surrounding envelope which will be at the wall potential. As will be seen later the difference in potential between the walls and the decaying plasma will not be more than of the order of tenths of a volt.

Now let some portion of the envelope be increased in potential with respect to the remainder. Then excess electrons will pour into that portion, causing the potential of the plasma to rise until once again the balance between loss of electrons and positive ions is attained. The plasma will now assume a potential slightly positive with respect to the most positive electrode with which it "makes contact." [An exception to this occurs when the area of the most positive electrode is so small that the normal electron diffusion current to it does not exceed the positive ion diffusion current to the entire boundary.] This property of decaying plasmas was demonstrated in a very simple fashion.

A tube was built in the form shown in Fig. 1. The filling was argon at 250$\mu$. It was connected in a circuit as shown in Fig. 2. The tube was fired by impressing a negative pulse on the cathode. The current to the probe as a function of time and $E_b$, following the interruption of the discharge, was measured by means of the scope across $R_b$ ($E_b$ is the probe battery potential). Two typical oscilloscope traces are shown in Fig. 3. The lower curve is for a case in which the probe is slightly positive with respect to the anode; i.e., $E_b-E_p>0$, ($E_p$ is the anode supply potential). The upper curve is for the case in which $E_b-E_p<0$. At a time $t_1$, the grid sheath extends across the 1 mm grid opening thus isolating the plasmas on both sides of the grid.[3] In Fig 3, $t_1$ is the time at which the kinks in the decay curves occur. For any value of $E_p$, $E_b$ could be set so that at some time $t>t_1$, the current to the probe was zero. Under this condition, the probe is at floating potential $E_f$. $E_p$ was varied over a range of $\pm 16$ volts on either side of ground potential and $E_f$ was determined in each case for $t>t_1$. The results are plotted in Fig. 4. It is seen that $E_f$ follows $E_p$ very closely.

The plasma potential $E_s$, is always slightly positive with respect to floating potential. The difference between the two is a function of the electron and ion temperatures. Since (as will be seen) both these temperatures are low for $t>t_1$, it follows that $E_s$ lie close to $E_f$ and therefore close to $E_p$, i.e., the space potential follows the potential of the most positive electrode, this being the anode in this case. For the case of Fig. 4, when $E_p=0$, $E_f$ appears to be about $-0.8$ volts. Since the contact difference of potentials between the various electrodes is not known, nothing can be said concerning the significance of this value.

In order to determine how rapidly the plasma potential follows that of the most positive electrode, the potential of the anode was varied by means of steep wave-front signal during the period $t>t_1$. It was found that equilibrium conditions (as observed on the scope) were always re-established within about $\frac{1}{4}$ microsecond. Since this is about the rise time of the pulses employed, it is impossible to estimate the time for equilibrium to be established. Very likely the times involved are deter-

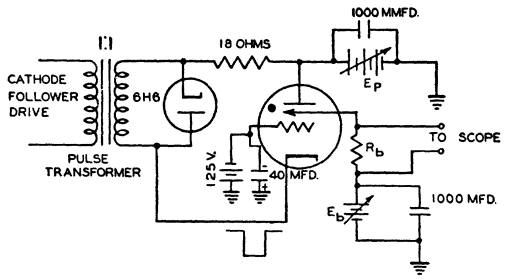


FIG. 2. Circuit for measuring floating potential of probe in decaying plasma.

FIG. 3. Decay currents to probe in tube of Fig. 1.

[3] The phenomenon of splitting of plasmas by the formation of sheaths across aperture openings is described by W. Koch, Zeits. f. Tech. Phys. **17**, 446 (1936).

mined primarily by electron mobility considerations and are thus less than $10^{-8}$ sec. for this particular tube.

## IV. THE DOUBLE PROBE METHOD (DPM)

The double probe method makes use of two probes, each similar to the single probe of the SPM. They are interconnected as shown in the circuit of Fig. 5. The potential $V_d$ is termed the differential voltage, and its associated current, $i_d$ the circuit current. The positive sense of these quantities is established by the arrow directions where we define positive current as the rate of flow of positive charge. Unless otherwise noted the circuit of Fig. 5 and its polarity convention will apply to all of the discussion which follows. In brief, the electron temperature will be determined from the way in which $i_d$ varies with $V_d$.

As with the SPM the DPM is based on the Boltzmann relation and the plasma-sheath properties of a gas discharge. In addition it is based on an application of Kirchhoff's current law which requires in this case that at any instant the total net current of positive ions and electrons flowing to the system from the plasma must be zero.

### Qualitative Treatment

As an aid in understanding the mathematical formulation, let us consider qualitatively how the system reacts for several different values of $V_d$. For simplicity, let us first assume that both probes are equal in area and that no contact potentials or differences in plasma potential from point to point exist. Furthermore, we assume that $V_d$ has no effect on the ion current to the system. This is very closely approximated in practice.

(*a*) $V_d=0$ (Fig. 6a).

Each probe will collect zero net current from the plasma and will ride at the same floating potential. The current $i_d$ must be zero since no net potential acts in the current loop. This condition corresponds to point 0 on the curve of Fig. 7.

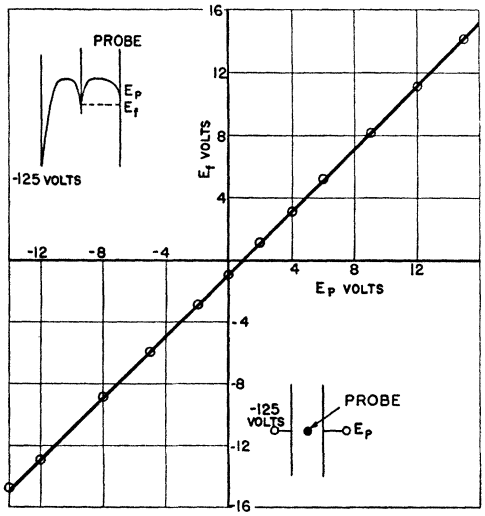


FIG. 4. Probe floating potential as function of anode potential for decaying plasma.

(*b*) $V_d$=small negative voltage (Fig. 6b).

The probe potentials with respect to the plasma must adjust themselves so that the basic current relations are still satisfied. The consideration of a few possibilities will show that the only way in which the system can satisfy all conditions is that it assume the potentials shown in Fig. 6b. Probe No. 1 moves closer to plasma potential and collects more electrons, and probe No. 2 moves away from plasma potential and collects fewer electrons. The extra electrons flowing to probe No. 1 pass through the circuit to make up the deficiency at probe No. 2. All conditions are again satisfied and the system is located at some point *b* on Fig. 7.

(c) $V_d$=somewhat larger negative voltage (Fig. 6c).

Probe No. 1 moves still closer to space potential and collects the entire electron current to the system since probe No. 2 is now so highly negative with respect to the plasma that no electrons can reach it. Half of the electrons reaching probe No. 1 now pass through the external circuit to probe No. 2. All conditions are satisfied and the system locates at some point *y* on Fig. 7.

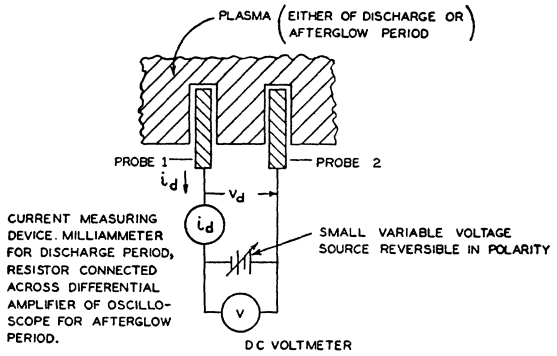


FIG. 5. Basic double probe circuit.

Further increase in the negative value of $V_d$ can cause no further change in the current distributions because probe No. 1 already collects a sufficient electron current to balance the entire positive ion current flowing to the system. Consequently probe No. 1 remains fixed with respect to the plasma and probe No. 2 goes negative along with $V_d$. We can speak of the latter probe as being saturated with respect to positive ions as the system moves along the flat portion *yx* of Fig. 7. In practice one finds that this flat portion has a slight slope as shown by the dotted portion *yx'*. This slow increase is due to an expansion of sheath thickness as the probe goes increasingly negative with respect to the plasma. This will be discussed in greater detail below.

The symmetry of the system will cause it to reverse the previous results when $V_d$ is positive, giving the

portion *ozw* or *ozw'*. The flat portion *zw* or *zw'* corresponds to positive ion saturation current to probe No. 1.

The total positive ion current to the system is simply the sum of the positive ion currents to both probes and so can be found by adding the magnitudes of the currents at $y$ and $z$, as symbolized by $i_{p_1}$ and $i_{p_2}$.

The electron current which flows from the plasma to probe No. 2 is simply the difference between the total space current and the positive ion current to this probe. Thus the electron current $i_{e_2}$ to probe No. 2 is given by

$$|i_{e_2}| = |i_d| - |i_{p_2}|. \tag{3}$$

The value of $i_{e_2}$ which corresponds to a voltage $V_d$ is illustrated graphically in the same figure.

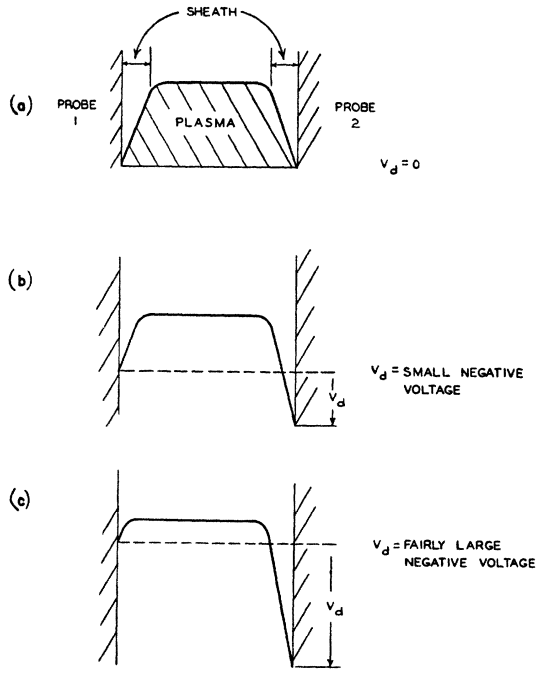


FIG. 6. Sample potential diagrams of the double probe method.

## V. TEMPERATURE DETERMINATION

### A. Logarithmic Plot Method

The generalized potential diagram for the system of Fig. 5 is shown in Fig. 8. The potentials $V_1$ and $V_2$ represent the voltages of the surrounding plasmas with respect to the corresponding probes. The potential $V_c$ represents any small difference in plasma potential which may exist between the regions surrounding the probes, plus the total contact potentials acting in the system. The other symbols are defined in the figure.

Since the net current to the system must be zero

$$i_{p_1} + i_{p_2} = \Sigma i_p = i_{e_1} + i_{e_2}.$$

Substituting the equivalents for $i_{e_1}$ and $i_{e_2}$ in terms of Boltzmann relation, we obtain:

$$\Sigma i_p = A_1 j_{0_1} \epsilon^{-\phi V_1} + A_2 j_{0_2} \epsilon^{-\phi V_2}, \tag{4}$$

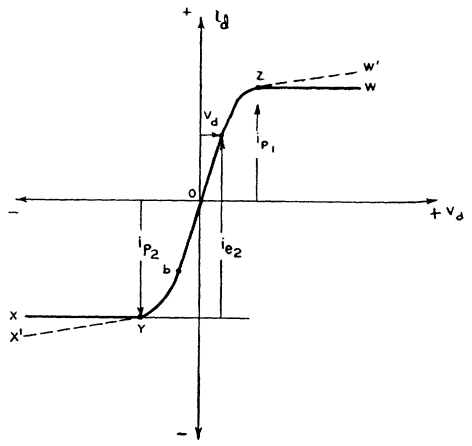


FIG. 7. Voltage-current characteristic of the double probe method.

where

$$\phi = e/kT_e = 11{,}600/T_e.$$

The potential diagram of Fig. 8 yields:

$$V_1 + V_c = V_2 + V_d \quad \text{or} \quad V_1 = V_2 + V_d - V_c. \tag{5}$$

Substituting (5) into (4) and rearranging, we obtain:

$$\ln[(\Sigma i_p/i_{e_2}) - 1] = -\phi V_d + \ln \sigma = \ln \Gamma, \tag{6}$$

where

$$\Gamma = (\Sigma i_p/i_{e_2}) - 1 \tag{7}$$

and

$$\sigma = (A_1 j_{0_1}/A_2 j_{0_2}) e^{\phi V_c}. \tag{8}$$

Thus the plot of ln $\Gamma$ against $V_d$ should yield a straight line whose slope is a measure of the electron temperature. This equation is seen to be similar in form to that used in the SPM except that in (6) one uses $\Gamma$ instead of the electron current. It is to be noted that the slope of (6) is essentially unaffected by any of the factors included in $\sigma$; *viz.*, probe areas, electron random current densities, difference in plasma potential between probes, and contact potentials. For an unambiguous determination of $T_e$, the random current densities should not change with probe current. This is much more likely to be the case with the DPM than with the SPM since the current drain can be hundreds of times smaller in the former case. Another important difference between the two cases is seen from Eqs. (2) and (8). We note that the constant term of the latter is free from any restricting dependence on the plasma potential. Thus we see that the DPM is inherently a more general method. It can be used during or after the discharge and even when the plasma potential varies with time.

Possible errors in this method require discussion. The values of $i_{p_1}$ and $i_{p_2}$ used were those at which the curve of Fig. 7 broke away from the saturated regions; (points $y$ and $z$ of Fig. 7). There are two possible sources of error present. In the first place, there is some uncertainty in the choice of points $y$ and $z$. To see how serious

this can be, trial points for $y$ and $z$ were chosen extending over a considerable range away from the obvious "break" points. It was found that when this was done, the end points of the log plot would deviate from the straight line defined by the central points. If one used the slope of the still well-defined straight central portion of the plot for determining the temperature, the values obtained did not vary significantly as the chosen values of $i_{p_1}$ and $i_{p_2}$ were moved around. The reason for this is quite simple. Any change in the selected value of the $i_p$'s, introduces a change (in the same direction) of the estimated value of $i_{e_2}$. It turns out that (except near $y$ and $z$) the significant quantity $[(\Sigma i_p/i_{e_2})-1]$ is inappreciably affected. Thus, one can safely say that this method is insensitive to small variations in the choice of $i_{p_1}$ and $i_{p_2}$.

A second possible source of error lies in the fact, that even in the region between $y$ and $z$ of Fig. 7, the ion current of each of the probes varies slightly due to

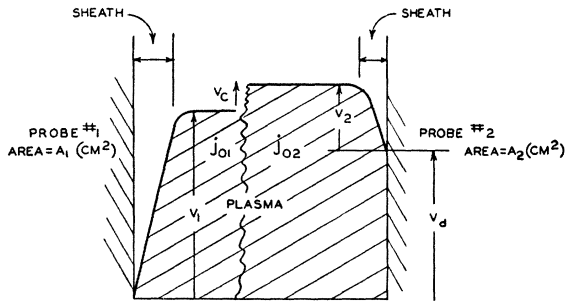


FIG. 8. General potential diagram for the double probe method.

$j_{01}$ = Electron space current in the plasma adjacent to probe No. 1.
$j_{02}$ = Electron space current in the plasma adjacent to probe No. 2.
$T_e$ = Electron temperature ( K) of the plasma.
$V_1$ = Probe to plasma potential probe No. 1.
$V_2$ = Probe to plasma potential probe No. 2.
$V_c$ = see text.

small changes in sheath thickness.[4] Strictly speaking, one should compute the positive ion current to each of the probes over the range $yz$ and use the sum of these in the log plot. This appears quite unnecessary and is, in fact, inconsequential, for the following reasons: (1) Unless the slope of the saturated ion current regions is considerable, the value of $\Sigma i_p$ can hardly change appreciably over the range $yz$. In any case, any actual and accepted change must be accompanied by a corresponding value for $i_{e_2}$. In that case for the reason cited in the second preceding paragraph, the effect on $(\Sigma i_p/i_e)$ will be small, since both $\Sigma i_p$ and $i_e$ change in the same direction in roughly the same ratio, (2) As one moves through the region between the knees, i.e., between $y$ and $z$, a change in $i_{p_1}$ tends to be compensated for by an opposite change in $i_{p_2}$, so that the true value of $\Sigma i_p$ remains approximately constant.

[4] The question of sheath thickness change is discussed more fully in the treatment of the "equivalent resistance method" below.

## B. Equivalent Resistance Method

Plotting Eq. (6) involves some laborious computation. It turns out that this can be avoided and $T_e$ determined very quickly from $i_d$ *vs.* $V_d$ plots. Equation (6) can be expressed as:

$$i_{e_2}=\Sigma i_p/[\sigma\epsilon^{-\phi V_d}+1]. \tag{9}$$

Taking the derivative of $i_{e_2}$ with respect to $V_d$ and evaluating at $V_d=0$, one obtains:

$$[di_{e_2}/dV_d]_{V_d=0}=(\Sigma i_p\phi\sigma)/(\sigma+1)^2. \tag{10}$$

Solving for $T_e$ and substituting for $dV_d/di_{e_2}$ its practical equivalent, $dV_d/di_d$, one obtains:

$$T_e=11{,}600\frac{\sigma}{(1+\sigma)^2}\left[\Sigma i_p\frac{dV_d}{di_d}\right]_{V_d=0}. \tag{11}$$

From (6) we can obtain:

$$\sigma=[(\Sigma i_p/i_{e_2})-1]_{V_d=0}.$$

For convenience we introduce the factor $G$ such that:

$$G=[i_{e_2}/\Sigma i_p]_{V_d=0}=1/(1+\sigma). \tag{12}$$

This factor $G$, which can be obtained directly from the current-voltage characteristic, obviates the need for calculating $\sigma$ from (8). Substitution of (12) into (11) yields:

$$T_e=11{,}600(G-G^2)[\Sigma i_p dV_d/di_d]_{V_d=0}$$
$$=11{,}600(G-G^2)R_0\Sigma i_p \tag{13}$$

where

$$R_0=[dV_d/di_d]_{V_d=0}. \tag{14}$$

The factor $R_0$ is denoted as the *equivalent resistance.* This gives the method its name. The simple relation Eq. (13) provides a rapid and convenient means of obtaining the electron temperature directly from the $V_d-i_d$ characteristic. The use of both (8) and (13) will be illustrated in the sets of experimental data which will follow.

Since, in the equivalent resistance method one makes use of the slope of the $V_d-i_d$ curve at only one point, viz. where $V_d=0$, it would be desirable to use the value of $\Sigma i_p$ corresponding to this point when computing $T_e$ from Eq. (13). A simple analysis (presented in the Appendix) indicates that one is usually justified in assuming that the rate of change of ion current along the sloping saturated portions of Fig. 7 is maintained in the regions between the knees. Manipulation of the basic equations of the DPM then yields the necessary relation between probe-space potential and $V_d$ which enables the course of $i_{p_1}$ and $i_{p_2}$ to be followed in the region between the knees. It is found that for all practical purposes, if the $V_d-i_d$ characteristic is reasonably symmetrical, one is safe in extending the lines $x'y$ and $w'z$ (see Fig. 7) 0.8 of the way into the line through $i_d=0$ and then horizontally the rest of the way. The

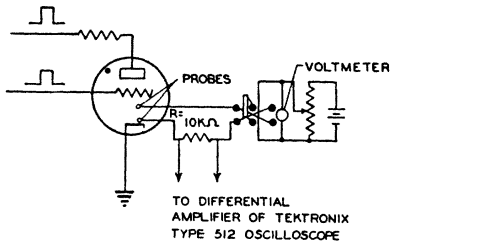


(A) CIRCUIT

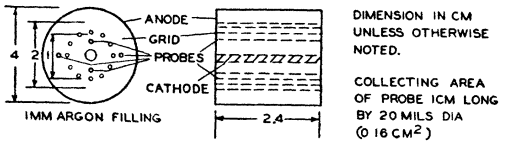


(B) EXPERIMENTAL TUBE # 4563-1

| | |
|---|---|
| ARC CURRENT DURING DISCHARGE | 50 MA |
| PLATE AND GRID PULSE MAGNITUDES | 150 VOLTS |
| PLATE AND GRID PULSE LENGTHS | 8 μS |
| GRID BIAS | 0 VOLTS |

(C) OPERATING CONDITIONS

FIG. 9. Tube and circuit for double probe studies of decaying plasma.

choice of this value is explained in the Appendix. From these extended curves one can obtain the value of $\Sigma i_p$ corresponding to $V_d=0$. (An illustration of this procedure is given in Fig. 11.) Experience has shown that if one fails to make this correction for $\Sigma i_p$ when employing the equivalent resistance method, but instead make of the positive ion currents corresponding to points $y$ and $z$ of Fig. 7, then the values for $T_e$ come out to be too large, but virtually never by more than 5 percent. Thus for rapid and approximate temperature determinations one can simply make use of $i_{p_1}$ and $i_{p_2}$ as determined from Fig. 7.

### C. The Intercept Method

In some cases the equivalent resistance method cannot be used owing to the fact that when $V_d=0$, one is operating in a region of positive ion saturation to one of the probes (i.e., in region $xy$ or $zw$ of Fig. 7). In that case another rapid method is possible which does not require the laborious computations of the logarithmic plot method.

By simple algebra Eq. (6) can be transformed into:

$$V_d=-\frac{1}{\phi}\ln\left[\left(\frac{1}{\sigma}\frac{\Sigma i_p}{i_{e_2}}-1\right)\right]. \tag{15}$$

Now let $V_d''$ be the value of $V_d$ which corresponds to $\Sigma i_p/i_{e_2}=D$, and let $V_d'$ be the value of $V_d$ which corresponds to $\Sigma i_p/i_{e_2}=F$. $D$ and $F$ are chosen arbitrarily. Then, substitution of these values in (15) and making use of the fact that $\phi=e/kT_e$, one can solve readily for $T_e$. The result is:

$$T_e=11{,}600\left[V_d''-V_d'\Big/\ln\left(\frac{F-1}{D-1}\right)\right]. \tag{16}$$

In the case of the intercept method it is found that, unless $V_d'$ and $V_d''$ are chosen too close to the knees, the value of $T_e$ determined is in excellent agreement with that obtained by the other methods.

In summary we can say that any error in the choice of $\Sigma i_p$ tends to be compensated, with the result that the error registered in $T_e$ will usually be 5 percent or less. It is obvious that the most certain values of $T_e$ are obtained in the cases where the flat portion slopes are a minimum. Comparison of corresponding temperatures obtained with different sets of probes, each set having different values of slopes in the flat portions, indicates that the 5 percent estimate is a reasonable one. This is also borne out by the close correspondence of temperatures as obtained from, (1) the logarithmic plot method based on $\Sigma i_p$ evaluated at the knees, and (2) the other two methods where $\Sigma i_p$ is computed from the interpolated values of $i_{p_1}$ and $i_{p_2}$.

It will be noticed that the mathematical treatment of the DPM is based on the potential diagram of Fig. 8 which represents an ideal case in which uniform electron densities and probe-plasma potentials exist along the probe surfaces. Such an ideal situation is not achieved in practice. However, it can be shown in a perfectly general and rigorous manner that non-uniform electron densities and probe-plasma potentials introduce no errors into the temperature measurements. Such non-uniformities, even when quite large, only introduce

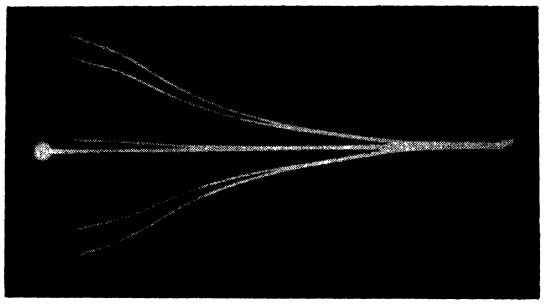

FIG. 10. Double probe current decay curves for tube of Fig. 9.

small corrections in the value of $\sigma$ as determined by Eq. (7). This deduction is consistent with the observation that the value of $\sigma$ determined by Eq. (7) is usually in close agreement with its value determined from either the log plot or the factor $G$.

In the case of probes used in tubes with oxide cathodes it has been found at times the deposition of barium onto the glass probe insulation (with subsequent leakage) causes the flat portions to have considerably increased slopes. A short application of a Tesla coil to the probe leads seems to burn out the barium, elimi-

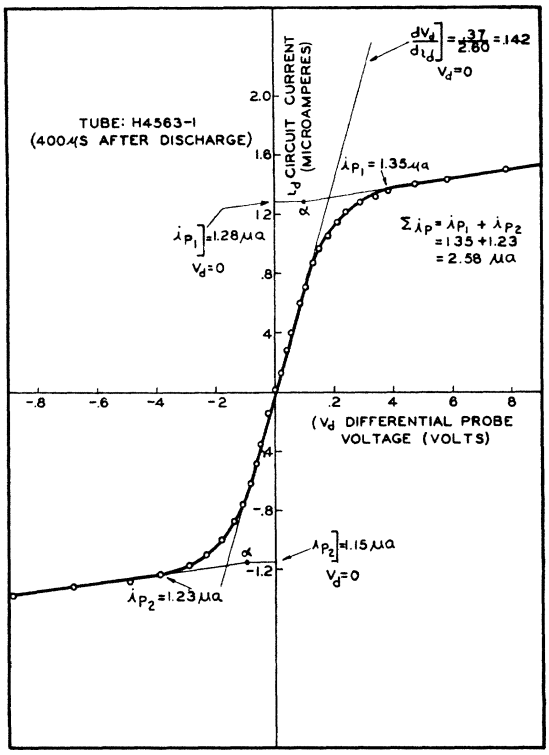


FIG. 11. Double probe current-voltage characteristic.

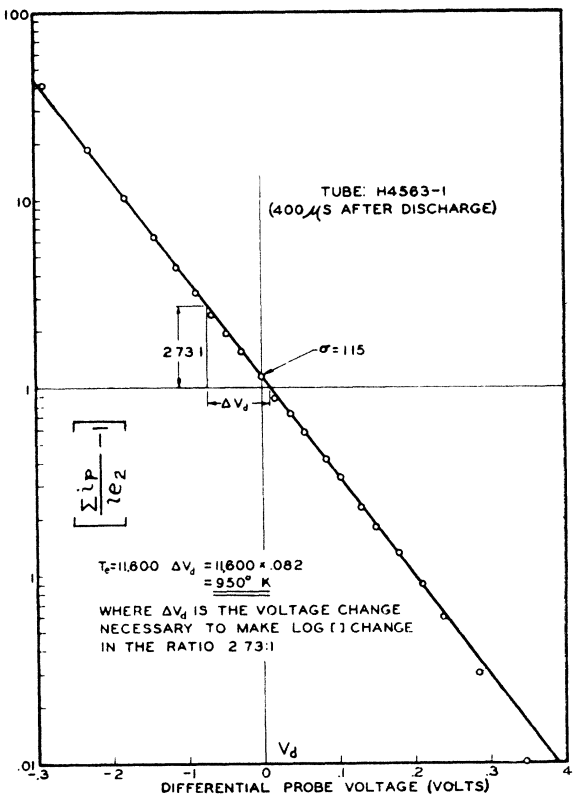


FIG. 12. Double probe temperature determination plot.

nating the leakage. Interestingly enough, the DPM seems to be sufficiently insensitive to error that the measurements made with leakage present (by the methods outlined above) agree within a few percent with those taken after the leakage has been eliminated.

## VI. ILLUSTRATIONS OF THE USE OF THE DPM

The presentation of the data which follow is mainly intended for the purpose of illustrating the use of the DPM and not as a detailed study of any particular phenomena which take place in the afterglow period.

The tests were carried out in the cylindrical triode shown in Fig. 9(B). Two sets of double probes were employed, one in the cathode-grid region and the other in the anode-grid region. The measuring set-up is shown in Fig. 9(A). (Only the cathode-grid probes are illustrated.)

The tube (containing Ar at 1 mm pressure) was fired by the simultaneous application of 8 $\mu$sec. pulses to grid and anode. The probe current was determined from deflections on a Tektronix No. 512 scope which has a balanced amplifier input. The operating parameters are presented in Fig. 9(C). Various cases illustrating the applicability of the DPM are presented below.

*Case 1.* Typical probe current decay curves for various values of $V_d$ are shown in Fig. 10. From these curves the current voltage characteristic can be obtained for any time. As an illustrative case, the data for 400 $\mu$sec. following the interruption of the discharge are plotted in Fig. 11.

The values of $V_d$ are corrected for the voltage drops in the resistor $R$. The values selected for the computation of $i_p$ are indicated in the same figure. The plot of the function $[(\Sigma i_p - 1)/i_{e_2}]$ against $V_d$ is presented in Fig. 12. The slope yields an electron temperature of 950°K. The temperature was also computed by means of Eq. (13) (the equivalent resistance method). The factor $G$ is found directly from Fig. 11 and is

$$G = [i_{e_2}/\Sigma i_p]_{V_d=0} = 1.12/2.43 = 0.463.$$

The value of 0.142 volts per $\mu$a for $R_0$ is computed from the slope of the characteristic of Fig. 6 at $V_d = 0$. The extensions of the flat portions[5] of the characteristic give the value of $\Sigma i_p$, at $V_d = 0$, as (1.15+1.28) or 2.43 $\mu$amp. Substituting the above values into (13) we get:

$$T_e = 11{,}600(0.249)(2.43)(0.142) = 1000°\text{K}.$$

This agrees quite well with the 950°K determined from the semilog plot.

The value of $\sigma$ computed from Eq. (12) and the above value of $G$ is 1.16. This agrees very well with the value of 1.15 determined by inspection of Fig. 12 at the point where $V_d = 0$. We can also compute $\sigma$ from

[5] The reason for this choice is discussed in the Appendix.

(8). Here

$$\sigma=[A_1 j_{0_1}/A_2 j_{0_2}]_{V_d=0}\epsilon^{\phi V_c}=(1)(1.28/1.12)(1.1)=1.24.$$

We assume that $j_{0_1}/j_{0_2}=i_{p_1}/i_{p_2}$ on the basis of the charge neutrality of the plasma. $\epsilon^{\phi V_c}=1.1$ since $V_c\simeq 0.01$ and $\phi=11.6$ (see Fig. 11). This value of $\sigma$ agrees reasonably well with the other two.

*Case 2.* As another illustration of the use of Eq. (8) and (13), for a case wherein the system is more dissymmetrical than in the previous case, we consider a set of data taken from a simple diode filled with 250$\mu$ of argon. The probes in this tube were equal in area and identical in size with those of the preceding case. The ar current was 200 ma and all data were collected at 100 $\mu$sec. after cessation of the discharge. The current-voltage characteristic is plotted in Fig. 13.

The values of the various factors are found from Fig. 13 and are

$$\Sigma i_p=10.7\ \mu\text{a},\quad [\Sigma i_p]_{V_d=0}=9.95\ \mu\text{a},$$
$$R_0=36{,}700\ \text{ohms},\quad G=0.401.$$

Then

$$T_e=11{,}600(0.240)(9.95)(0.0367)=1015^\circ\text{K}.$$

The log plot, shown in Fig. 14 yields a concurrent value of 1055°K. It is interesting to note that the values of $\sigma$ again check, their values being (*a*) 1.55 from log plot, (*b*) 1.50 from *G*, (*c*) 1.51 from Eq. (7).

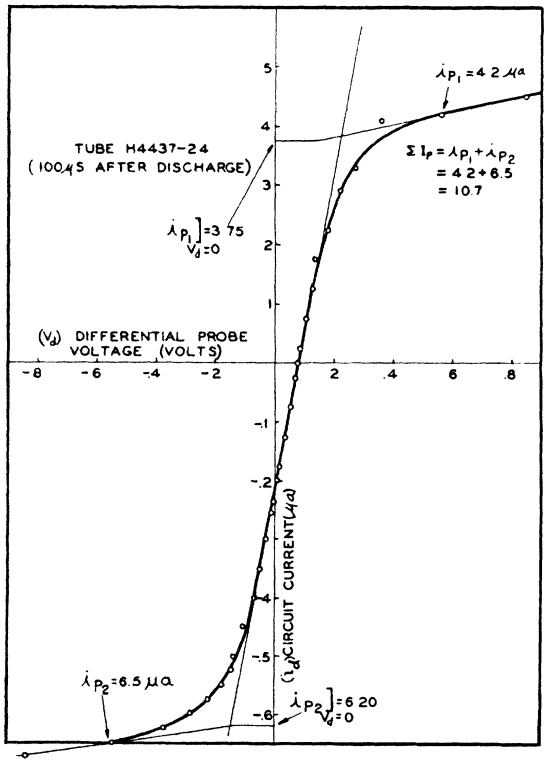


FIG. 13. Double probe current-voltage characteristic.

## VII. DISCUSSION OF EXPERIMENTAL RESULTS

A serious question arises regarding whether or not temperature determinations have a basis in reality. The concept of an electron temperature is permissible only if the electrons have a Maxwellian distribution. The method here described samples only a small fraction of the electrons present, the electrons collected by the probes being only those which have velocities sufficient to overcome the ever present retarding fields at the probes. The range of electrons sampled can be extended by making tubes with probes of dissimilar size.

It is of interest to determine what fraction of the electrons are sampled in one of the cases studied above. Consider Case 1, whose results are presented in Figs. 11 and 12. An approximate expression for floating potential $V_f$ (with respect to space potential) is given by:[6]

$$V_f=-(kT_e/2e)\ln(T_{em}/T_pM). \qquad (17)$$

Then for the case of Figs. 11 and 12, $T_e=950^\circ$K. For $M$ we use the mass of the argon atom. We assume that $T_p$ is the gas temperature which was about 350°K for this case. Then from Eq. (17) $V_f=0.50$ volts. Since $i_{p1}\simeq i_{p_2}$, the probes must be close to $V_f$ when $i_d=0$. Then from the Boltzmann relation, the ratio of electron

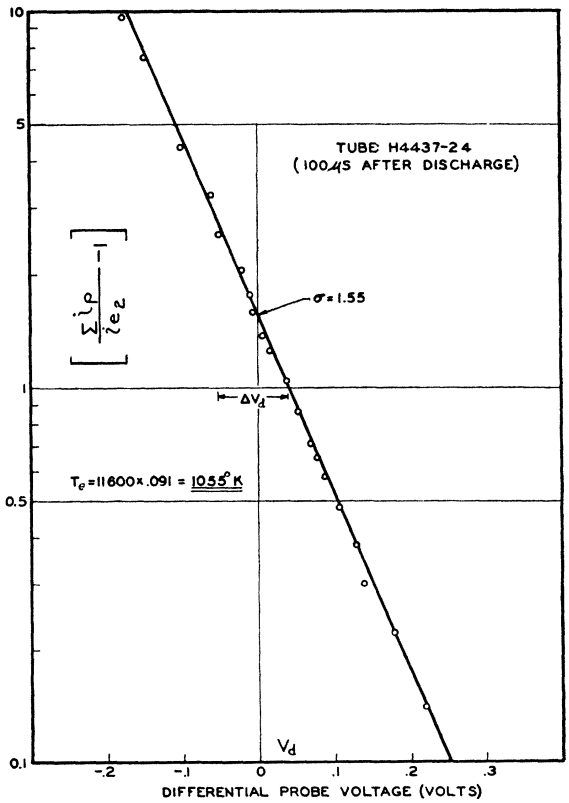


FIG. 14. Double probe temperature determination plot.

[6] L. B. Loeb, *Fundamental Processes of Electrical Discharge in Gases* (John Wiley and Sons, Inc., New York, 1939), first edition, p. 242.

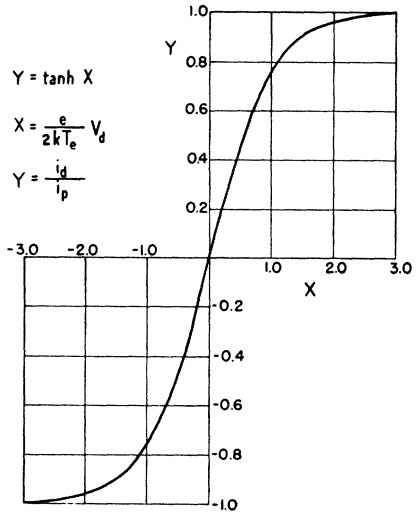


FIG. 15. Ideal double probe current-voltage characteristic.

current density at the probe to the random current density in the plasma near the probe (when the probe potential is $V_f$) is given by:

$$j_d/j_0 = e^{-(eV_f/kT)} = e^{-(11,600/950)(0.50)} = 0.0021.$$

From Fig. 11 we see that the measurements extend to points where the current to either probe becomes about double the above value. Thus the maximum value assumed by $j_d/j_0$ in this case is about 0.005. Thus less than the top 1 percent of the electrons are sampled in this case.

In other tubes than those described here, up to 5 percent of the electrons were sampled by means of probes with area ratios of 25. In these cases, too, the results always corresponded to Maxwellian distributions. It may obviously represent a dangerous extrapolation to conclude from the properties of this small sample that the electron velocity distribution is completely Maxwellian.

## VIII. FURTHER CONSIDERATIONS OF THE SPM AND THE DPM

It may appear that the single probe can be employed in the fashion of the double probe by considering the single probe as constituting one of a double probe pair and the remainder of the system as constituting the other probe of the pair. This is actually possible only in certain special cases.

From the earlier description of the DPM we see that regardless of the value of $V_d$ (the difference in potential of the probes) the space potential in the plasma is unaffected by changes in $V_d$. The plasma is dominant in determining its own potential as well as that of the floating probes. The potential of the latter is determined by that of the plasma and the condition of equality of electron and ion currents to the probe system.

This is not the case for the SPM. The probe or electrode potentials for this case can affect the plasma potential in such a way as to alter the quantities being measured. If a hot cathode is present, then the use of a positive probe may give rise to oscillations during the afterglow period. This is an undesirable state of affairs as the measuring device affects the quantity it is designed to measure. If a hot cathode or other copious electron source is not present (as in the case of a cold cathode discharge, or for the isolated anode-grid region plasma of case 3 above), then it is possible to use a single probe combined with the other electrodes as a double probe system.

## IX. ANALYTICAL EXPRESSIONS FOR $i_d$ AND $i_e$

Let us consider a symmetrical double probe system in which: (1) the probes are identical, (2) the random current density at both probes is equal, (3) the contact emf between the probes is zero, and (4) the space potential near both probes is the same. Then from Eq.

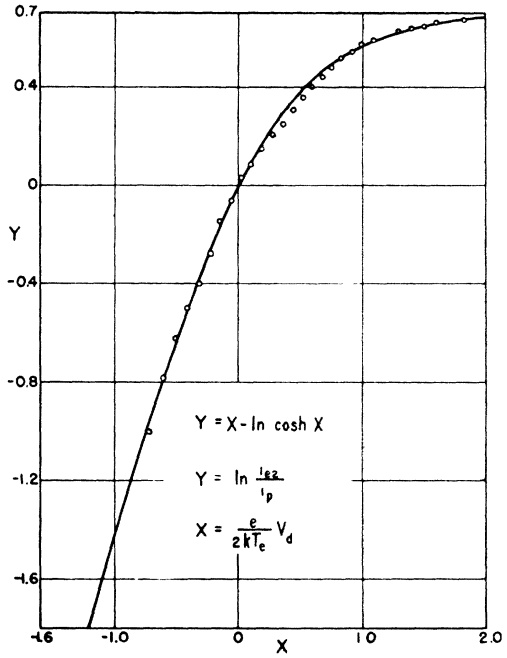


FIG. 16. Theoretical and experimental electron current plots for double probe method.

(8) $\sigma = 1$. Then from Eq. (6)

$$\Sigma i_p/i_{e_2} = 1 + e^{-\phi V_d}. \tag{18}$$

For this symmetrical case, $i_{p_1} = i_{p_2} = i_p$. Then: $\Sigma i_p = 2i_p$, where $i_p$ is the positive ion current to either probe. Making use of this relation and the fact that $i_{e_2} = i_d + i_p$, we can transform Eq. (18) into:

$$i_d/i_p = \tanh(\phi V_d/2). \tag{19}$$

A plot of this function is given in Fig. 15. It is seen to have just the shape of the observed data. (See Figs. 11 and 13.)

Equation (19) above can be written as:

$$2[i_{e_2}/\Sigma i_p]=i_{e_2}/i_p=2/(1+e^{-\phi V_d})$$
$$=\exp(\tfrac{1}{2}\phi V_d)/\cosh(\tfrac{1}{2}\phi V_d).$$

Then:

$$\ln(i_{e_2}/i_p)=\tfrac{1}{2}\phi V_d-\ln\cosh(\tfrac{1}{2}\phi V_d). \quad (20)$$

A plot of Eq. (20) is given in Fig. 16. The values of $\ln(i_{e_2}/i_p)$ were computed for a set of experimental data and the points plotted on Fig. 16. The agreement between theory and experiment is agreeably good.

Reifman and Dow[2] have plotted the quantity $\ln(i_e/i_p)$ for measurements in the ionosphere. Their double probe consisted of the nose and a portion of the body of a rocket. From their curve they conclude that the observed electron distribution is not Maxwellian. Since the shape of their observed curve is similar to ours, it is not possible to account for their conclusion. The shape of the $\ln(i_e/i_p)$ should not be altered qualitatively even for a non-symmetrical structure such as they employed.[7]

## X. DETERMINATION OF ELECTRON AND ION DENSITIES AND OF WALL POTENTIAL

Neither the SPM nor DPM are suited for the determination of the electron density $n_e$ in decaying plasmas. This arises from the fact that the plasma potential "rides" with the probe when the latter is run upward (i.e., in a positive direction) in potential. As a consequence, it is impossible to saturate the electron current to the probe unless its area is extremely small. In the Langmuir SPM it is the saturated electron current (corresponding to the bend in the current voltage characteristic) which is used to compute the electron density.

The situation is not completely hopeless, however. In order to determine $n_e$ and $n_p$, it is merely necessary to set a value on one unknown, the positive ion temperature $T_p$. This is an exceedingly fortunate situation, since the value of $T_p$ in the decaying plasma is undoubtedly very close to $T_g$, the gas temperature. This follows from the fact that even though the electron temperature may still (in some cases) be considerably above gas temperature, the kinetics of the impacts of the ions with electrons and gas molecules is such that it is the temperature of the latter which will dominate in determining the ion temperatures. In addition, as will be seen, $n_e$ and $n_p$ vary as the square root of $T_p$. Thus, errors in selecting a value for $T_p$ will have a much smaller effect on the values of $n_e$ and $n_p$. We set:

$$j_p=n_p e c_{Av}, \quad (21)$$

where $c_{Av}$ is the average drift velocity of the ions. In the decaying plasma, where the space-charge fields are extremely small, $c_{Av}$ must be due almost entirely to the outward motion from the plasma into the sheath arising from the random motion of the ions. In that case $c_{Av}=\frac{1}{4}\bar{c}_p$, where $\bar{c}_p$ is the ion velocity averaged over a Maxwellian distribution. Then:

$$n_p=4j_p/e\bar{c}_p, \quad (22)$$

where $j_p$ is the random ion current density, but:

$$j_p=i_p/A_s, \quad (23)$$

where $i_p$ is positive ion current to probe, and $A_s$ is sheath area.

Estimates made by the method of Langmuir and Mott-Smith[1] indicate that at the points $y$ and $z$ of Fig. 4, the positive ion current to the probe is space-charge limited but that the sheath area may be appreciably larger than the probe area.

Making the substitution $\bar{c}_p=1.87\times10^{-8}(T_p/M)^{\frac{1}{2}}$ we obtain:

$$n_p=(1.34\times10^{27}/A_s)i_p(M/T_p)^{\frac{1}{2}}, \quad (24)$$

where $M$ is the mass of a positive ion.

Let us apply this to the case of Fig. 11. For that case, $M(\text{argon})=6.65\times10^{-23}$ g, $i_p=1.35\times10^{-6}$ amp., $T_p=350°\text{K}$. Then

$$n_p=(8.0\times10^8/A_s)\ \text{ions/cm}^3. \quad (25)$$

To determine $A_s$ we make use of the space-charge-limited current equation for cylindrical diodes:

$$i_p=14.66\times10^{-6}(m_e/M)^{\frac{1}{2}}(LV^{\frac{3}{2}}/\Gamma\beta^2),$$

where $V$ is the difference in potential between the probe and plasma. For this case $L=1$ cm, $\Gamma=0.025$ cm, $i_p=1.35\times10^{-6}$ amp. Then

$$\beta^2=1.62V^{\frac{3}{2}}. \quad (26)$$

To obtain $V$, we recall first that when the probe is at wall potential ($i_d=0$) its potential with respect to the plasma (as was computed above) is 0.50 volt. As $i_d$ varies from zero in Fig. 11 to the saturation value of $i_{p_1}$, $i_{e_2}$ changes by a factor of about 2 (this is readily obtained from Fig. 12). The probe-space potential must then decrease by an amount determined from the Boltzmann relation:

$$0.5=\exp[(11{,}600/950°\text{K})\Delta V],$$

or

$$\Delta V=-(950/11{,}600)\times0.693\cong-0.06\ \text{volt}.$$

Then:

$$V=(0.50-0.06)=0.44\ \text{volt}.$$

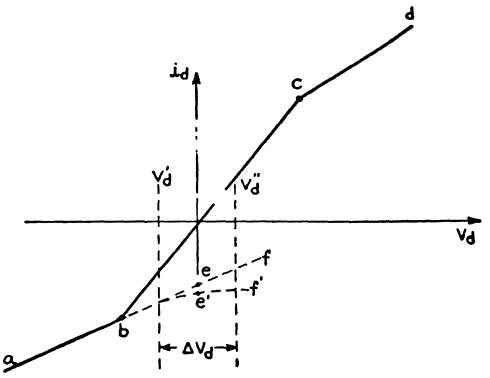


FIG. 17. Idealized double probe characteristic.

[7] Kojima and Takayama, J. Phys. Soc. Japan 4, 349 (1949) have recently described a slightly different method for using double probe data which yields temperature figures very close to those obtained by the methods here described.

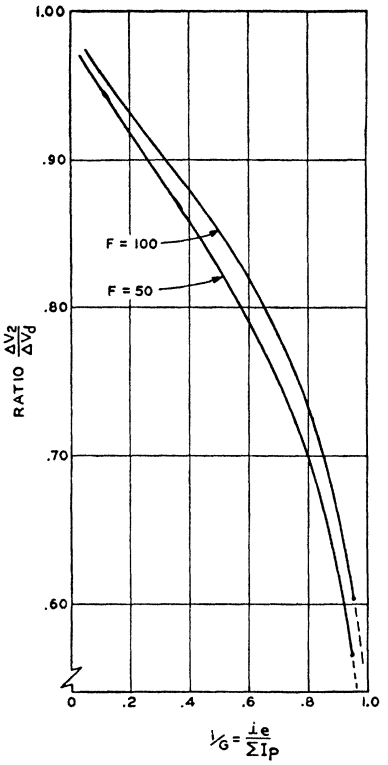


FIG. 18. Relation between space potential and differential potential.

Then from Eq. (26):

$$\beta^2=1.62\times0.29=0.47.$$

Then:

$$\Gamma_s/\Gamma_0=1.75,$$

where $\Gamma_s$ and $\Gamma_p$ are respectively the sheath and probe radii. Then:

$$A_s=1.75A_p=1.75\times0.16=0.28\ \text{cm}^2.$$

Substituting this value in (25) there results:

$$n_p=2.9\times10^9\ \text{ions/cm}^3.$$

From the equality of electron and ion density, we have immediately

$$n_e=2.9\times10^9\ \text{electrons/cm}^3.$$

The random electron and ion current densities can now be obtained from Eq. (21) using the proper value of $\bar{c}$ in each case.

## APPENDIX

### Variation of Positive Ion Current to Probes with Probe Potential

In the equivalent resistance method for temperature determination it was necessary to know the value of the ion current to the probes at $V_d=0$. This cannot be determined directly from the $V_d-i_d$ characteristic. We shall now present a crude analysis showing how the desired quantity may be calculated.

Consider an idealized DPM $V_d-i_d$ characteristic as shown in Fig. 17 with purposely exaggerated slopes for the ion saturation regions. These slopes arise from the change in sheath thickness with change in voltage across the sheath.

Along the saturated portions *ab* (or *cd*) a change in $V_d$ results in an identical change in the value of $V_2$ (the potential of probe No. 2 with respect to the plasma as illustrated in Fig. 8), since there is no change in the electron and positive ion current distribution as shared by the two probes. This is no longer the case as we move beyond *b* into the electron collection region.

We are interested in how $i_{p_2}$ (the positive ion current to probe No. 2 varies with $V_d$ in the region to the right of *b* in Fig. 17. To a sufficiently good approximation, the positive ion current in this region is given by the well-known space-charge-limited equation for cylindrical diodes:

$$i_{p_2}=cV_2^{\frac{3}{2}}/\Gamma_p\beta^2, \tag{27}$$

where $c$ is a constant, $\Gamma_p$ is the probe radius. Equation (27) neglects the effect of ion initial velocities, and of the effect of the electrons in the sheath. These cannot have any serious influence, however. A long series of computations for the ranges of current and voltage of interest showed that for the cases we are concerned with, $i_{p_2}$ varies linearly with $V_2$ to the right as well as to the left of *b*. Thus if changes in $V_2$ were equal to those of $V_d$, the $i_{p_2}$ characteristic in the electron flow region would be obtained by simply extending the line *ab* through *e* and *f* as shown in Fig. 17. Actually since $V_2$ changes less rapidly than $V_d$ in this region, the $i_{p_2}-V_d$ characteristic looks more like the line *abe'f'*. We must determine the value of $i_{i_2}$ at *e'*.

If in Eq. (6) we substitute for $i_{e_2}$ its equivalent value $A_2j_{0_2}e^{-\phi V_2}$ and solve for $V_2$ we obtain:

$$V_2=-\frac{1}{\phi}\ln\frac{\Sigma i_p}{[\sigma e^{-\phi V_d}+1]A_0j_{0_2}} \tag{28}$$

Now let $V_d$ take on two values $V_d'$ and $V_d''$ as shown in Fig. 17. Let the values of $V_2$ corresponding to these two values of $V_d$ be $V_2'$ and $V_2''$, respectively. We wish to determine $\Delta V_2=V_2'=V_2''$. Then:

$$\Delta V_2=-\frac{1}{\phi}\ln\left[\frac{\sigma e^{-\phi V_d''}+1}{\sigma e^{-\phi V_d'}+1}\right]. \tag{29}$$

For the situation corresponding to $V_2'$ and $V_d'$ let

$$\Sigma i_p/i_{e_2}=\Sigma i_p/[A_0j_{0_2}e^{-\phi V_2}]=F,$$

and similarly let $\Sigma i_p/i_e$ corresponding to $V_2''$ and $V_d''$ be denoted by $G$. Equation (29) then becomes:

$$\Delta V_2=-(1/\phi)\ln(G/F). \tag{30}$$

From Eq. (6) and the definitions of $F$ and $G$ we can obtain:

$$\Delta V_d=V_d''-V_d'=-(1/\phi)\ln[(G-1)/(F-1)]. \tag{31}$$

Combining (30) and (31) we obtain:

$$\frac{\Delta V_2}{\Delta V_d}=\frac{\ln(F/G)}{\ln[(F-1)/(G-1)]}. \tag{32}$$

As an origin, we choose a value for $F$ corresponding to $V_d$ close to the point *a* of Fig. 17 where detectable electron current flows. Experimentally it is observed that a definite deviation from the straight line region of the $V_d-i_d$ characteristic is observable when

$$50<\Sigma i_p/i_{e_2}<100.$$

As a consequence, the value of $\Delta V_2/\Delta V_d$ was computed from Eq. (32) for $F=50$, and $F=100$. The results are plotted in Fig. 18.

For the case of a symmetrical $V_d-i_d$ characteristic,

$$1/G=i_{e_2}/\Sigma i_p=0.5$$

when $V_d=0$. It is seen from Fig. 18, that for this condition $\Delta V_2/\Delta V_d\simeq0.8$. Thus in practice, to find the value of $i_{e_2}$ corresponding to $V_d=0$, one merely extends the region *ab* of Fig. 17 linearly to a point 0.8 of the way from *b* to *e*. The point $\alpha$ in the figure gives the desired value of $i_{p_2}$ to be used in computing $\Sigma i_p$ in the equivalent resistance method for determining $T_e$. If the $V_d-i_d$ characteristic is not symmetrical one must make use of Fig. 18 to determine how far beyond the linear region *ab* one must extrapolate in order to determine $i_{e_2}$.

In the curve of Fig. 11, which is very close to being symmetrical, the figure 0.8 was used.

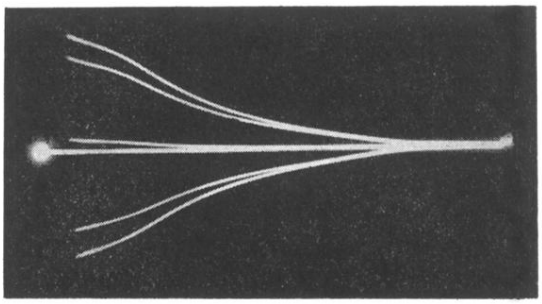

FIG. 10. Double probe current decay curves for tube of Fig. 9.

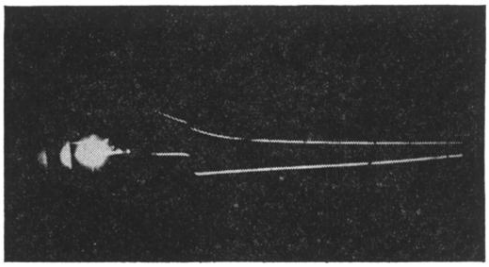

FIG. 3. Decay currents to probe in tube of Fig. 1.